Mortar Radiocarbon Dating: Preliminary Accuracy Evaluation of a Novel Methodology

6 AUTHORS, INCLUDING:

Fabio Marzaioli
Second University of Naples
56 PUBLICATIONS **316** CITATIONS

Carmine Lubritto
Second University of Naples
109 PUBLICATIONS **829** CITATIONS

Isabella Passariello
Second University of Naples
32 PUBLICATIONS **285** CITATIONS

Filippo Terrasi
Second University of Naples
262 PUBLICATIONS **2,935** CITATIONS

Mortar Radiocarbon Dating: Preliminary Accuracy Evaluation of a Novel Methodology

Fabio Marzaioli,*,[†] Carmine Lubritto,[†] Sara Nonni,[‡] Isabella Passariello,[†] Manuela Capano,[§] and Filippo Terrasi[†]

[†]INNOVA, Centre for Isotopic Research on Cultural and Environmental Heritage and Dipartimento di Scienze Ambientali, Seconda Università degli Studi di Napoli, Caserta, Italy

[‡]Centro di Ricerca per le Scienze Applicate all'Ambiente e ai Beni Culturali, Università la "Sapienza" Roma, Roma, Italy

[§]INNOVA, Centre for Isotopic Research on Cultural and Environmental Heritage and Dipartimento di Studio delle Componenti Culturali del Territorio, Seconda Università degli Studi di Napoli, Santa Maria Capua Vetere, Caserta, Italy

S *Supporting Information*

ABSTRACT: Mortars represent a class of building and art materials that are widespread at archeological sites from the Neolithic period on. After about 50 years of experimentation, the possibility to evaluate their absolute chronology by means of radiocarbon (^{14}C) remains still uncertain. With the use of a simplified mortar production process in the laboratory environment, this study shows the overall feasibility of a novel physical pretreatment for the isolation of the atmospheric $^{14}CO_2$ (i.e., binder) signal absorbed by the mortars during their setting. This methodology is based on the assumption that an ultrasonic attack in liquid phase isolates a suspension of binder carbonates from bulk mortars. Isotopic (^{13}C and ^{14}C), % C, X-ray diffractometry (XRD), and scanning electron microscopy (SEM) analyses were performed to characterize the proposed methodology. The applied protocol allows suppression of the fossil carbon (C) contamination originating from the incomplete burning of the limestone during the quick lime production, providing unbiased dating for "laboratory" mortars produced operating at historically adopted burning temperatures.
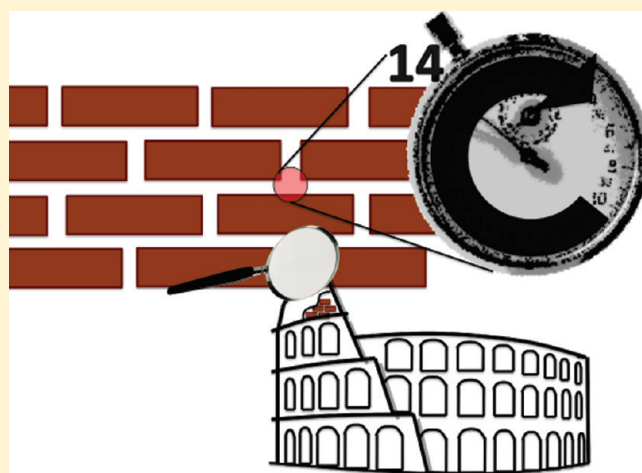
To date, radiocarbon chronology of archeological sites is mostly based on the dating of organic materials found at the study site. Hence, significant gaps may be introduced between ^{14}C dates and the real age of the site or the studied event.[1] Using mortars (MOs) to evaluate the age of artifacts represents a sensitive improvement in radiocarbon dating methodology of archeological events. Mortars and plasters were extensively used to construct floors, walls, roads, aqueducts, and even to create art. As a result, these materials are virtually ubiquitous at archeological excavations since 7000 B.C.[2] They also represent a valid tool to assess the chronology of artifacts when they were found on bedrocks or lie on different strata or can be used as a survey tool to preliminarily evaluate the opportunity to proceed with excavations if the site matches its supposed age.[3]

Aerial mortars were, historically, produced by a sequential production phase: (i) limestone (LS) was burnt in high temperature (800−1000 °C) furnaces to produce calcium oxide (quick lime) in the calcination process:

$$CaCO_3 \rightarrow CaO + CO_2$$
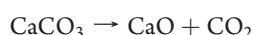
(ii) quick lime (QL) was slaked in water to produce calcium hydroxide (slaked lime) and preserved under water excess (y) forming a lime putty:[4]

$$xCaO + (x + y)H_2O \rightarrow xCa(OH)_2 + yH_2O$$
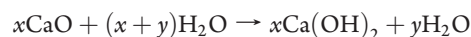
(iii) slaked lime (SL), mixed with inert materials, was used undergoing hardening because of the absorption of atmospheric CO_2[5] and loss of water:

$$Ca(OH)_2 + CO_2^{atm} \rightarrow CaCO_3 + H_2O$$
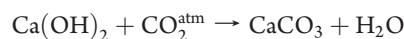
In principle the unique source of carbon present in the mortar is the CO_2 absorbed during the manufacture of the building. Hence, dating of MOs can be performed because CO_2 absorption records the time of mortar setting and this latter is negligible

A

dx.doi.org/10.1021/ac1027462 | *Anal. Chem.* XXXX, XXX, 000–000

with respect to ^{14}C half-life (5730 $\pm$ 40 years[6]). Unfortunately the presence of different contamination sources can lead to contradictory results.[5,7−10] Several studies identify the inefficient suppression of the contamination originating from the original carbonate residues surviving the burning of the LS one of the main reasons for the systematic errors in mortar dating methodology.[5,7,9−11]

A large effort has been devoted by the scientific community to find a reliable ^{14}C dating of mortars, and time has been spent in attempting an efficient isolation of the atmospheric CO_2 signal, preserved in the binder phase of the mortar carbonate, from other carbonaceous sources, whose coexistence in the mortar matrix leads to a significant aging effect on the measured ages. The current state of the art approaches point to the binder signal isolation mainly by means of a partial acid attack. This methodology, proposed first by Delibrias and Labeyrie,[7] is based on the evidence of a different reaction rate for the carbonates as a function of their diagenesis (i.e., binder carbonates react faster than limestone lumps[7,9,12]) and widely applied leading to a series of contradictory results.[1,3,5,7−9] Partial acid attack was recently reviewed suggesting the isolation of a series of CO_2 partly digested fractions reflecting the isotopic signal absorbed during their diagenesis.[13] To our knowledge, the unique alternative to this methodology is based on the attempt to separate the binder carbonates by a combined mechanical/physical procedure[5,11,14] based on the laboratory isolation of calcite crystals produced as the consequence of atmospheric CO_2 absorption.

An important aspect regarding the protocol validation for mortar dating is the characterization of their stable isotopes ratios.[10,15] Van Strydonck et al.[10] and Nawrocka et al.,[11] in both procedures (i.e., chemical and physical/mechanical), suggest a stable isotope ^{13}C-back correction (see section 1 of the Supporting Information for details) for the measured ages attempting to suppress the effects of dead C contamination. This procedure is based on the main assumption of the absence of C isotopic discrimination (fractionation) along mortar processing. To our knowledge, most of the studies analyzing this process use the isotopic fractionation experienced by atmospheric CO_2 during the absorption to characterize the mortar setting. Pachiaudi et al.[15] as well as Kosednar-Legenstein et al.[16] found a measurable fractionation effect during this phenomenon. This effect was interpreted as an overall Rayleigh type distillation process.[17]

In order to (i) maintain the concept of the isolation of a fraction from the mortar preserving the isotopic signature of the atmospheric CO_2 and (ii) allow a reliable dating without performing partial acid digestions and several radiocarbon measurements of complex interpretation, we decided to investigate a modified mechanical/physical procedure for mortar radiocarbon dating.

To avoid combined effects, we performed an accuracy evaluation of the proposed methodolgy on a simplified version of mortars, influenced by only one (i.e., unburnt LS C, ref 10) of the supposed sources of uncertainty affecting accurate chronology reconstructions by means of mortars. In order to preliminarily evaluate the accuracy of the procedure in dead C suppression and to characterize the entire process, in this paper we simulated a simplified mortar production protocol (i.e., no aggregates were added to the mortar) in the laboratory environment. This test allowed

us to primarily verify the agreement of the isolated binder signal (^{13}C and ^{14}C) with the measured atmospheric one and, secondarily, to better characterize the mortar production process with a specific emphasis on verified isotopic fractionations.

■ EXPERIMENTAL SECTION

Synthetic Mortar Production. Laboratory synthetic mortar production simulates the original mortar sequential production phases with the exception of the addition of inert materials. During our simulation, we also tested the influence of different temperatures on the quick lime manufacturing. In detail, a carbonaceous rock of about 30 kg mass was chosen to synthesize the laboratory mortar. Scraps (n = 3, randomly sampled from LS) were powdered by means of a rotary tool and used for the characterization of the initial matrix in terms of % C, mineralogy (i.e., XRD), ^{13}C and ^{14}C.

WIth the aim to to simulate the quick lime production phase, six different (not pulverized) LS fragments of approximately 15 g underwent burning in a muffle furnace capable of reaching up to 1100 °C. In detail, each of the originary 6 samples was burnt for 1 h at 700, 800, 900, 1000, and 1100 °C and for 1.5 h at 700 °C. The muffle thermal cycle was controlled by means of a temperature controller allowing the oven to reach the set temperature in approximately 1 h, maintaining it for the programmed time (e.g., 1 h), and switching off the oven when the set time elapsed. Produced QLs (QL 700, QL 800, QL 900, QL 1000, QL 1100, QL 700_1.5) were subsequently pulverized and underwent % C, ^{13}C, and ^{14}C analyses.

A stoichiometric excess of deionized water was added to the pulverized qiucklimes (about 4 g) in beakers to simulate the slaked lime product phase. With the aim to increase the yield of the reaction over the experimental periods and simulate an aging of the $Ca(OH)_2$ crystals, the beakers were ultrasonically treated for 60 min. It is well documented how excess water as well as low temperatures increase the dissolution of CO_2 in the aqueous strong alkaline environment leading to a general speeding up of the CO_2 absorption process (carbonatation) by the slaked lime.[16,18] For 3 weeks, samples were kept at 4−6 °C to increase the CO_2 dissolution process and for 2 successive weeks at 25 °C to facilitate mortar carbonate hardening in a temperature controlled environment. The produced MOs (MO 700, MO 700_1.5, MO 800, MO 900, MO 1000, MO 1100), after pulverization, underwent % C, ^{13}C, and ^{14}C analyses, and MO 700 and MO 900 were analyzed by SEM.

Laboratory CO_2 Air Sampling. During the whole carbonatation phase (5 weeks), two spot samples of laboratory air CO_2 (1st and 4th week) were sampled to have an isotopic reference to be compared to our mortar binder signal. CO_2 was purified by other atmospheric gases, according to Bertolini et al.,[19] by means of a dynamic cryogenic system, capable of isolating CO_2 from other air gases with no observed fractionation.

Isolation of the Atmospheric CO_2 Signal from the Mortar Carbonate. Our protocol is based on a modification of the procedure described by Nawrocka et al.[11] It is based on the assumption that binder carbonates are characterized by an easily breakable aggregation structure (i.e., by means of ultrasonication attacks). Our working hypothesis is that this step operates the binder signal isolation from the unburnt LS

residuals by breaking the binder minerals and originating a suspension of carbonates characterized by a slower sedimentation velocity ($v_{s\infty}$) because of their smaller average diameter (d_p).[20]

In details, (i) bulk mortar breaking: bulk mortars (5−10 g) were submerged in liquid nitrogen for about 5 min and rapidly moved into an oven at 80 °C. After at least three cycles, raw materials were crushed by means of gentle hammering. (ii) Suspension production: thermally broken materials, still containing the binder and the LS residues, underwent ultrasonication in an excess of deionized/decarbonated water for 30 min in a beaker generating a suspension (SU) of binder. (iii) Suspension isolation: the liquid phase of the produced suspension was gently siphoned in 50 mL Falcon centrifuge tubes and centrifuged for 5 min at 8.5 krpm to separate the suspension from the water medium. The water filling the tubes was gently removed, and the SU fraction was dried overnight at 70 °C. The protocol isolated suspensions (SU 700, SU 700_1.5, SU 800, SU 900, SU 1000, and SU 1100) underwent ^{13}C and ^{14}C analyses, and SU 700 and SU 900 were analyzed with SEM.

% C Measurements. % C determinations were performed by means of a Thermo 1112 Flash elemental analyzer. Samples were weighed ($n = 3$) in tin cups. Empty tin cups and calibration and check standards were run together with unknown samples.

Isotope Analyses. ^{13}C and ^{14}C analyses were performed by means of a complete orthophosphoric acid (H_3PO_4) attack. Ampules for isotope analyses[22] containing the carbonate materials and a frozen excess of H_3PO_4 [85%] were evacuated ($<10^{-3}$ mbar) and detached from the line after isolation. H_3PO_4 digestion was developed in an oven (85 °C) for a period of 2 h. Produced gases underwent cryogenic purification by means of a vacuum line[18] to separate evolved CO_2. Carbon dioxide was split in two subaliquots: (i) for the stable isotope ratio determination and (ii) for the radiocarbon sample pretreatment/measurements.

Stable isotope analyses were performed by means of a Thermo Delta Plus isotope ratio mass spectrometer directly on the CO_2 via dual inlet using a lab tank as reference. In order to correct for eventual procedure induced fractionations, three internationally recognized carbonate reference materials (IAEA C1, C2,[23] and NBS 19) were used for the normalization procedure. ^{13}C abundances are expressed according to the δ notation[24] as permil of excess with respect to the Peedee belemite (PDB) primary reference material:

$$\delta^{13}C = \frac{(^{13}C/^{12}C)_{sample} - (^{13}C/^{12}C)_{PDB}}{(^{13}C/^{12}C)_{PDB}} \times 1000$$

Radiocarbon analyses were performed on the graphite developed from the CO_2 following the zinc reduction process.[21] With the aim to check for the entire procedure accuracy, reproducibility, and induced background, IAEA C1 (background), IAEA C2 (normalization), and several check standards were prepared following the same procedure. Graphite samples were measured by means of the CIRCE-AMS system for the measurement of radiocarbon isotopic ratios.[25] For the purposes of this study, we present ^{14}C data, according to Stuiver and Pollach,[26] in both pMC (percent of modern carbon), mostly used for geochemical

scopes and to express the post 1950s ages, and radiocarbon (R.C.) age.

$$pMC = \frac{\left.(^{14}C/^{13}C)_{sample}\right|_{-25‰}}{\left.(^{14}C/^{13}C)_{OXI}\right|_{-19‰} e^{\lambda(y - 1950)}} \times 100$$

$$^{14}F = \frac{\left.(^{14}C/^{13}C)_{sample}\right|_{-25‰}}{\left.(^{14}C/^{13}C)_{OXI}\right|_{-19‰}}; \quad R.C.age = -8033 \ln {}^{14}F$$

In both measured isotopic ratios of the sample and the primary standard (OXI) are corrected for isotopic fractionation to a $\delta^{13}C$ value of −25 and −19‰, respectively. Moreover, when pMC notation is used, the OXI isotopic ratio is scaled for decay to 1950. In this study, some ^{14}C measurements are converted in R.C.ages, via calibration, in calendar ages and expressed in A.D. years, reporting B.C. dates as negative A.D. values. Calibration of R.C.ages was performed by means of Calib 6.0[27] software; other radiocarbon data (i.e., $^{14}F > 1$) were directly converted in A.D. ages by means of CALIBomb.[28] All these dates are reported by means of the probability-weighted averages of the medians of the calibrated ranges, while error bars represent 1 and 2σ maximum and minimum ranges.

Partial Acid Attack. With the aim to improve the suppression efficiency on the unique dead C contaminated SU samples, we applied a partial acid digestion (SU 700_PA and SU 700_1.5_PA). In our case, by knowing that for the 700 suspensions there was an amount of dead carbon varying between 16 and 25% left (see later and Figure 3), we decided to process 100 g of suspension with the stoichiometric amount of acid necessary to digest only 10% of the C. At the end of the CO_2 purification, the residual liquid phase was checked for the neutral pH.

XRD/SEM analyses. About 10 g of material was sampled and grinded to a minimum particle diameter of 270 mesh. The powder was loaded in the tray of a Phillips PW 1800 X-ray diffraction instrument, and the spectra were acquired by means of Co K-alpha radiation.

SEM images were taken at the Surfaces Thin Films and Nano Structures (STN) Laboratory in the Physics Department at the University of L'Aquila with a LEO 1503 apparatus equipped with a field effect gun. The beam was typically operated at 1 kV.

Data Analysis. Replicated measurements are reported as weighted averages using the error of the weighted average (internal error) as dispersion index. If the χ^2 test of the H_o hypothesis: "the internal error is not statistically different from the standard error (external error) of the sampled population" is not verified at a level of significance of 95%, the standard error is used for dispersion estimation purposes. The usage of different position/dispersion indicators will be specified in parentheses.

Comparison of the data will be performed by means of a t test for the means. The results of the comparison indicate no difference between the means if the level of agreement of the test ($1 - \alpha$) lies within 0.05 and 0.95.

C

Table 1. % C, δ^{13}C and pMC Measured on the Laboratory Produced Quick Limes and Laboratory Mortars

	sample ID	% C	δ^{13}C (mil)	pMC (%)
quick limes	QL700	8.6 ± 0.3^a	2.36 ± 0.02	2.30 ± 0.06
	QL700 1.5	8.9 ± 0.2^a	2.64 ± 0.01	0.83 ± 0.03
	QL800	0.38 ± 0.03^a	-9.3 ± 0.7^a	N.M.^{b}
	QL900	0.34 ± 0.02^a	-22.92 ± 0.04	N.M.^{b}
	QL 1000	0.143 ± 0.003^a	-16.52 ± 0.05	N.M.^{b}
	QL1100	0.20 ± 0.03^a	-18.70 ± 0.04	N.M.^{b}
laboratory mortars	MO 700	10.3 ± 0.1^a	-1.88 ± 0.02	20.3 ± 0.1
	MO 700 1.5	9.6 ± 0.2^a	-2.01 ± 0.02	21.9 ± 0.2
	MO 800	3.7 ± 0.3^a	-14.9 ± 0.01	94.3 ± 0.4
	MO 900	5.4 ± 0.4^a	-15.15 ± 0.01	97.9 ± 0.4
	MO 1000	5.2 ± 0.9^a	-21.98 ± 0.02	97.4 ± 0.4
	MO 1100	4.4 ± 0.7^a	-19.2 ± 0.02	100.2 ± 0.4

^{a} Values represent weighed mean $\pm$ standard error on n = 3 samples. ^{b} N.M. stands for not measured.

RESULTS AND DISCUSSION

LS Characterization. The initial limestone carbonate showed an average % C content of $10.2 \pm 0.2\%$ (mean $\pm$ standard error), a δ^{13}C of 2.9 ± 0.2‰, and a pMC of $0.12 \pm 0.05\%$. All measurements were in agreement with the values expected for a sedimentary carbonate: (i) % C around 12% (the theoretical % C value for the pure calcite ($CaCO_3$)), (ii) δ^{13}C comparable to the isotope signature of cretaceous carbonates ($+1$ to $+3$‰[29,30]), and (iii) depleted radiocarbon abundances, related to the ancient age of the carbonaceous material. XRD analysis evidenced how the initial material was composed of low magnesium calcite crystals. Low Mg contents of the original material avoid the possibility of formation of magnesic mortars characterized by slower carbonation velocities[31] not compatible with our experimental times.

QL Production Process. The calcination process appeared very sensitive (i.e., % C, δ^{13}C) to the temperatures of the applied treatment (Table 1). QL produced at 700 °C, independent of the applied time of combustion (QL 700 and QL 700_1.5), is depleted with respect to the original carbonate. For these samples, the observed degree of C depletion indicates inefficient calcinations (about 80% of LS C is still present in the samples). QL produced at temperatures ranging between 800 and 900 °C are sensitively depleted with respect to MO 700 series but slightly enriched with respect to the ones produced in the 1000–1100 °C range. It can be noted how efficient calcination happens (i.e., less than 1% of the LS C remains in the QLs) only for temperatures ≥ 800 °C.

$MgCO_3$ dissolves in the 450–520 °C range while $CaCO_3$ dissolves in the 700–900 °C range.[32] Thermal dissolution of calcite happens at 898 °C at 1 bar of pressure of pure CO_2, and the calcination temperature decreases with the lowering of the CO_2 concentration.[33] This evidence fits the observed threshold behavior of calcination well, with the small C loss up to 800 °C probably attributable to the selective $MgCO_3$ thermal dissolution.

Measured QL δ^{13}C values (Table 1) were in statistical agreement with the measured LS only for calcination temperatures of 700 °C. For calcination temperatures higher than 700 °C, a strong depletion in the ^{13}C signature is observable. Calcination temperatures higher than 700 °C induce a sensitive isotopic fractionation in the residual/lost carbon. We observed a

preferential loss of the heavier stable isotope of carbon leaving the residual $CaCO_3$ depleted in ^{13}C. This process is better known as the inverse isotope effect,[34] in opposition to the normal fractionation predicting enrichment in the heaviest isotope composition of the residue of calcination.

Our measurements raise some questions about the literature-suggested ^{13}C back correction.[10,11] Indeed, this correction is based also on the assumption of preservation of the isotopic signature of the LS in the MO even after calcination, implying the absence of isotopic fractionation during the production of QL. Measured fractionations constitute a good explanation for previous bibliographic evidence of depleted δ^{13}C mortar carbonates values until levels lower than the atmospheric CO_2 level.[11,16] These observations were justified by supposing the usage of aggregates for MO production with a C isotopic signature different from the one occurring in the cretaceous[11] or by hypothesizing a carbonation with depleted biogenic CO_2.[16] To our knowledge, no studies have been published underlying a possible isotopic fractionation during the calcination as a possible explanation for the observed degrees of depletion in the mortar matrixes.

The measured radiocarbon signals on QL 700 and QL 700_1.5 (Table 1) were strongly depleted in ^{14}C. These values were in agreement with the one measured on the three replicates of the original LS ($0.12 \pm 0.05\%$). A t test comparison of $1.1 \pm 0.8\%$ (weighted average on the pMCs of the QL 700 and QL 700_1.5) with this latter confirms the agreement between these measurements. Then, hereafter, we use this value as a representative of the QL ^{14}C signature independent of the calcination temperature applied.

Carbonation Process. Laboratory CO_2 absorption over the experimental period leads to a mass increase (data not shown) ranging between 34 and 37% for the QLs produced at temperatures ≥ 800 °C. For the 700 °C QL series, the mass increases only from 8 to 20%. The theoretical mass increase for the complete reaction of carbonation (i.e., 79%) implies a yield of carbonation close to 50% for the QL produced at T higher than 700 °C and much slower for not completely calcinated samples.

The % C (Table 1) measurements on MO replicates confirm the overall success of the carbonation procedure: all measured MO % C values were significantly enriched with respect to the respective QLs. The % C reached by the MO 700 and MO 700_1.5 was not statistically different from the % C of the LS

Table 2. Fraction of Limestone Residual C Constituting the Mortar Carbonate (χ_1), δ^{13}C, and pMC of the Binder Phase of the Mortar Evaluated by Means of the Isotopic Mass Balance

sample ID	χ_1	δ^{13}C binder	pMC binder
MO 700	0.83 ± 0.03	−22 ± 4	113 ± 32
MO700_1.5	0.92 ± 0.02	−54 ± 14	255 ± 97
MO 800	0.10 ± 0.01	−15.6 ± 0.1	105 ± 2
MO 900	0.06 ± 0.01	−14.62 ± 0.05	105 ± 1
MO 1000	0.03 ± 0.01	−22.13 ± 0.04	100 ± 1
MO 1100	0.05 ± 0.01	−19.22 ± 0.02	105 ± 2

carbonate. The % C of other MO carbonates were significantly depleted with respect to the 700 °C series but constant independent of the temperature of the QL production

The % C data reported in Table 1 can be used to estimate some important details about the carbonation process. It is possible to evaluate (Table 2) the fraction of limestone residual C (χ_1) composing the mortar carbonate by performing the ratio between the % C measured on the QL and the relative produced MO. It must be noted how, because of the incomplete carbon removal of the LS C during calcination, the χ_1 characterization of MO 700 and MO 700_1.5 is sensitively higher than other MOs. These characteristics make these samples (i) a material not easily usable for constructive uses given the low hardening ratio related to the low CO_2 absorption; (ii) an extremely high dead C contaminated material; (iii) a less sensitive tool for the binder δ^{13}C/pMC estimations (higher uncertainties affecting the mass balance approach (see the next paragraph for details)). SEM analyses on the laboratory produced mortars (Figure 1A and B) clearly confirm their different nature, with the MO 700 characterized by a coarser and more angular structure than MOs produced from the LS calcinated at 900 °C.

It appears that carbonatation differentiates the two subsets of mortars: the first produced by the carbonatation of the QL 700 series characterized by low atmospheric CO_2 absorption rates (i.e., most of the C constituting these samples is ascribable to LS), higher % C, and preservation of the crystalline aspect of the initial carbonate. The second by QLs produced at temperatures higher than 700 °C is characterized by higher rates of CO_2 absorption, lower % C and the development of regular surfaces.

δ^{13}C and pMC values (Table 1) also confirm the absorption of CO_2 from the laboratory atmosphere, being both different by their respective δ^{13}C and mean pMC (1.1 ± 0.8%) of the QLs. MO 1000 and MO 1100 were found comparable to the previously observed δ^{13}C of laboratory synthesized mortars.[15]

Evaluating the Binder Isotopic Signature and Carbonation Fractionation. Assuming that C composing our synthetic mortar carbonate (m) is ascribable to two sources, (i) the LS carbonate (l) survived the burning for the quick lime production, (ii) the carbonate forming the binder (b) produced by the carbonatation of the slaked limes is characterized by a characteristic carbon isotopic fingerprint ^{i}F (i.e., δ^{13}C or pMC). With the hypothesis of a homogeneous dispersion of the two source signals, it is possible to evaluate the isotopic content of the binder present in the mortar (see section 2 of the Supporting Information for details) by applying the isotopic mass balance (IMB) using as input data the χ_1 (Table 2), the δ^{13}C, and pMC of the QL and of the MO (Table 1, see section 3 of the Supporting Information for details). Assuming all the values (Table 2) are representative of an independent replicate set for the evaluation

of the δ^{13}C and pMC of the binder, we estimate them to be, respectively, −19 ± 6‰ and 102 ± 25%.

The evaluation of both the ^{13}C and ^{14}C signatures of the binder is affected by an uncertainty of about 1 order of magnitude higher than the atmospheric variability (see later) over the reference period addressable to MO 700 and MO 700_1.5 (see the previous paragraph). Rejection of these values gives an evaluated δ^{13}C and pMC signature of the binder phase of −19 ± 2‰ and 102 ± 1%, respectively, not altering the average values but significantly affecting their index of dispersion.

Over the whole carbonatation period, CO_2 constituting the laboratory atmosphere was sampled and the estimated δ^{13}C and pMC were, respectively, −11 ± 1‰ and 100 ± 2%. It can be noted how the measured values are evidence of a sensitive fossil C source that can significantly affect the depleted measured isotopic values of CO_2 with respect to the clear air values.

The binder estimated IMB δ^{13}C should exactly preserve the signature of the atmospheric CO_2 if no isotopic fractionation is observed during carbonation, while binder radiocarbon estimations should appear in agreement with the atmosphere independent of the presence/absence of this fractionation. In our case, the t test between the measured ^{13}C values (i.e., atmosphere −11 ± 1‰ and binder −19 ± 2‰) indicates a small fractionation. This finding was in agreement with a previous study[16] simulating the absorption of CO_2 from a pure $Ca(OH)_2$/water solution at different CO_2 pressures. In this study, the observed ^{13}C $CaCO_3$/CO_2 fractionation was found to decrease as soon as the partial pressure of CO_2 approaches the atmospheric values. The observation of a measurable fractionation process during MO carbonatation agrees also with Pachiaudi et al.[15] but points out the possibility of shallower atmosphere/mortar C fractionation with respect to this study.

IMB evaluated binder pMC values are in agreement with the measured atmosphere $^{14}CO_2$. In this case, the significance of the absence of a difference between the atmosphere and the binder is valid. This last result is a clue to the good practice of the ^{14}C measurement and correction procedure applied at the CIRCE laboratory.

Binder Signal Isolation Procedure. Considering the suspension phase ^{13}C values (Figure 2) as independent replicates of the same phase (i.e., the binder), we evaluate the suspension signal in −14.7 ± 0.3‰. The data variability affecting the suspension ^{13}C measurements is very narrow, compatibly with the directly measured atmospheric $^{13}CO_2$ and underlies a good reproducibility of the applied procedure for the binder signal ^{13}C isolation. SU values lie between the atmospheric value (−11 ± 1‰) and the IMB evaluated binder signal (−19 ± 2‰, see previous paragraph for details). Comparison of SU with IMB δ^{13}C values, with the two deviations of the order of 2−3σ, indicates the fair effectiveness of dead C suppression provided by the applied isolation procedure for all the types of MO analyzed in this study.

SEM analyses on the isolated suspensions (Figure 1C,D) do not show any particular difference between the samples independent of their history, confirming the apparent effective suppression of the LS fossil signal in agreement with the results found by application of the ^{13}C tool.

Suspension ^{14}C signals converted in calendar ages show a different behavior from what is evidenced by looking at ^{13}C (Figure 3). Radiocarbon, in fact, evidences a different behavior in the efficiency of the dead C contamination suppression. Our procedure gave reliable results (comparable to the atmosphere CO_2 and IMB ^{14}C values) only when calcination temperatures

E

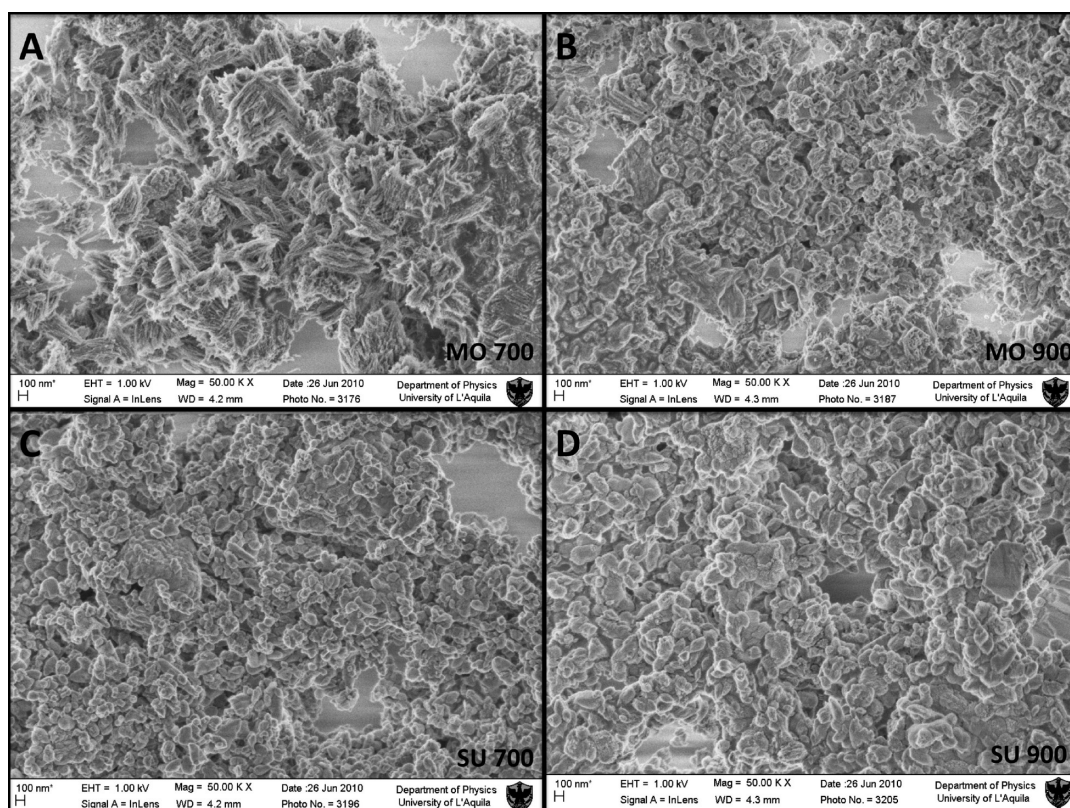dx.doi.org/10.1021/ac1027462 |*Anal. Chem.* XXXX, XXX, 000–000

Figure 1. Scanning electron microscopy images of the laboratory produced mortars (i.e., MO 700 (A) and MO 900 (B)) and the suspensions isolated by the same samples (i.e., SU 700 (C) and SU 900 (D)).
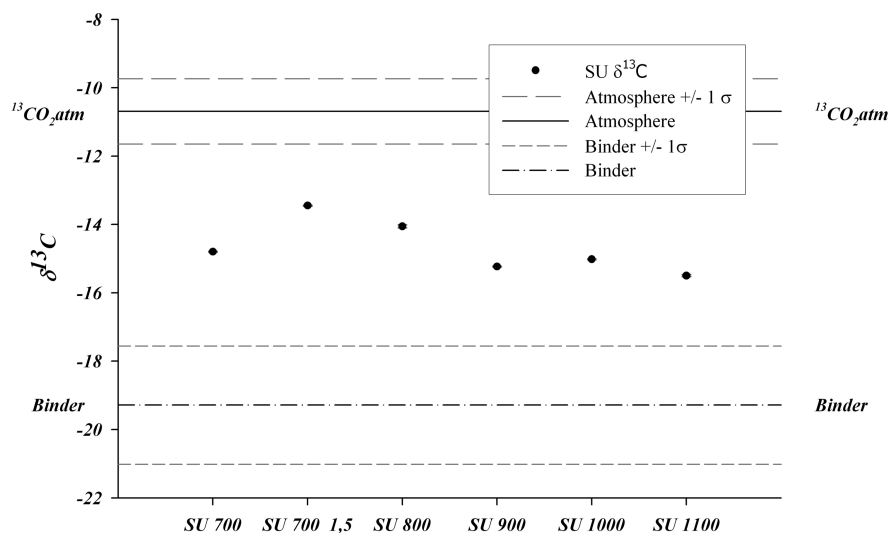

Figure 2. Measured $\delta^{13}C$ values of the suspension isolated from the mortars following this study proposed isolation procedure compared with the isotopic signature of the laboratory air CO_2 (directly measured) and the binder signal evaluated by means of the mass balance approach with the rejection of MO700 and MO700_1.5 outliers (see the text for details).

were ≥ 800 °C. For temperatures of quick lime production lower than 800 °C, most of the C constituting the mortars (i.e., 83 and 92%, Table 2) was of limestone origin so that our procedure fails in the efficient suppression (i.e., 100%) of the original limestone residues leading to an aging effect of about 2000 years for SU 700 and 1200 years for SU 700_1.5. Radiocarbon measurements performed on these suspensions together with the pMC values measured on the atmosphere and quick limes (i.e., $1.1 \pm 0.8\%$)

can be used to evaluate the relative contribution of the residual limestone carbonate (χ_{old}) by an ulterior application of an IMB (Figure 3, see the Supporting Info for details). Residual C fractions in statistical agreement with zero show no significant difference from the atmospheric CO_2 value. These measurements allow us to estimate the suppression efficiency of the proposed procedure by comparing the χ_{oldC} of the SU with the χ_{l} present in the laboratory mortar carbonate. Suppression
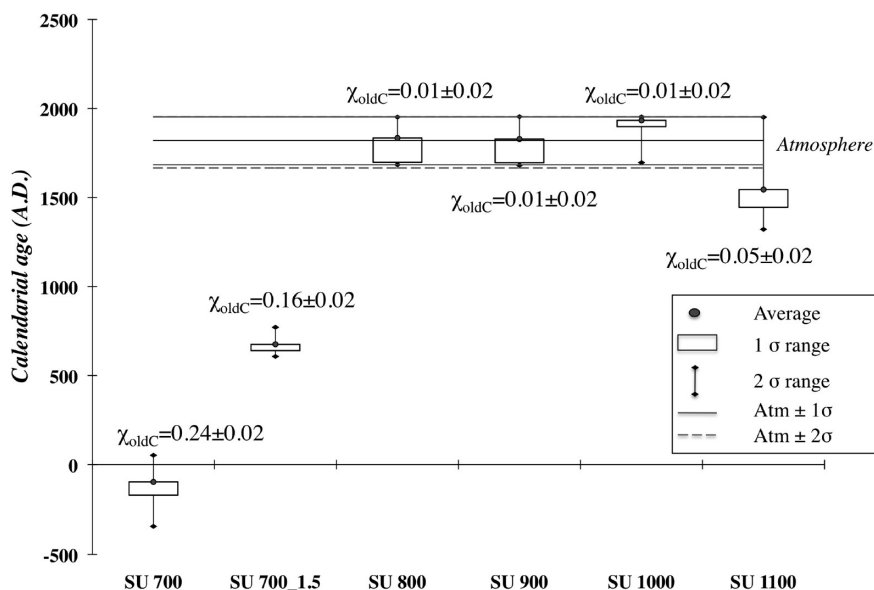
Figure 3. Calibrated radiocarbon ages (expressed in A.D., assigning B.C. dates as negative A.D. values) measured on the suspension phases extracted by the laboratory produced MO carbonates and laboratory atmospheric CO_2. Weighted averages and $1-2\sigma$ ranges are reported for each of the measured values together with the fraction of C of limestone origin (χ_{oldC}) still present in the sample.

efficiencies measured were not compatible with 100% only for suspensions originating from MO 700 and 700_1.5 (i.e., $72 \pm 2\%$ and $83 \pm 2\%$). These materials represent a sort of outlier in the commonly applied production process of mortars because it is commonly accepted that because calcination efficiently happens at temperatures in the $800-1000\ °C$ range,[3,34,35] they were not used for constructive uses.

The sensitivity of the applied methodology based on ^{14}C measurements is about 3-fold better than that based on [13]C. These results suggest using the ^{13}C tool just as an exploratory (not constraining) analysis preceding the more sensitive and expansive ^{14}C analysis of the isolated suspensions.

The partial acid digestion applied to the SU 700 and 700_1.5 samples (i.e., SU 700_PA and SU 700_1.5_PA) yielded 78.6 ± 0.3 and 81.2 ± 0.7 pMC, respectively, showing no improvement in the dead carbon suppression. In our case, as also observed by van Strydonk et al.[10] in the case of very powdery mortars, partial acid digestion was not effective for the isolation of the atmospheric CO_2 preserved in the binder.

■ CONCLUSIONS

This study explores the possible application of the radiocarbon dating methodology to evaluate mortar ages by means of a novel physical procedure aiming to isolate the binder from other carbonate sources commonly leading to sensitive aging effects on the absolute chronology evaluation of studied sites. This goal was achieved by reproducing a simplified mortar production process in the laboratory that performed even at different calcination temperatures and characterizing its intermediate phases aiming to estimate reference values useful for procedure accuracy evaluations. The laboratory mortar production process allowed us (i) to show sensitive ^{13}C isotopic fractionation during the limestone calcination according to the treatment temperatures, (ii) to underline shallow ^{13}C isotopic discrimination during the QL carbonation. Both findings raise some questions about the literature suggested ^{13}C-backcorrection hypothesizing a lack of isotopic discrimination over the mortar production procedure. In this

framework it is important to notice how, aiming to dating purposes, this correction would result in higher values of the conventional age, implying inaccuracy of the correction model.

Produced mortars, after their characterization, were processed for the isolation of the binder signal and analyzed. All measured ^{13}C values on the suspension phases were in slight agreement with the atmospheric $^{13}CO_2$ of the laboratory air. Radiocarbon ages were in agreement with the atmospheric reference for applied temperatures of calcination higher than 700 °C. Only when the QL is produced at temperatures lower than 800 °C, a sensitive dead C effect is observable. The applied partial acid digestion did not improve the aging effect introduced in these sample processings. Such disagreement, anyhow, should not influence the protocol applicability to archeological samples because calcination and subsequent carbonation is not efficient at these temperatures. Given the overall successful character of the proposed methodology in the dead C suppression of unburnt limestone origin, a second phase of testing will be performed on real field mortars. Comparison of the observed results with other independent chronology estimations will be used to further refine the methodology.

■ ASSOCIATED CONTENT

ⓢ Supporting Information. Additional information as noted in text. This material is available free of charge via the Internet at http://pubs.acs.org.

■ AUTHOR INFORMATION

Corresponding Author
*Address: Via Vivaldi, 43 81100, Caserta, Italy. Phone and fax: +390823274814. E-mail: fabio.marzaioli@unina2.it.

■ REFERENCES

(1) Ringbom, A.; Hale, J.; Heinemeier, J.; Lancaster, L.; Lindroos, A. *Am. Sci.* **2003**, *91* (2), 130–137.

(2) Bensted, J. In *Cement: Past, Present and Future*; Dartford Greenwich University Press: Dartford, U.K., 1997.

(3) Rech, J. A.; Near, E. *Archaeol.* **2004**, *67* (4), 212–219.

(4) Rodriguez-Navarro, C.; Hansen, E.; Ginell, W. S. *J. Am. Ceram. Soc.* **1998**, *81* (11), 3032–3034.

(5) Folk, R. L.; Valastro, S. *J. Field Archaeol.* **1976**, *3* (2), 203–208.

(6) Godwin, H. *Nature* **1962**, *195* (4845), 984–984.

(7) Delibrias, G.; Labeyrie, J. *6th International Conference on Radiocarbon and Tritium Dating*, Pullman, WA, 1965; p 344.

(8) Stuiver, M.; Smith, C. S. *6th International Conference on Radiocarbon and Tritium Dating*, Pullman, WA, 1965; p 338.

(9) Baxter, M. S.; Walton, A. *Nature* **1970**, *225*, 937–938.

(10) Van Strydonck, M.; Dupas, M.; Dauchot-Dehon, M.; Pachiaudi, Ch.; Marechal, J. *Radiocarbon* **1986**, *28* (2A), 702–710.

(11) Nawrocka, D.; Michniewicz, J.; Pawlyta, J.; Padzur, A. *Geochronometria* **2005**, *24*, 109–115.

(12) Sonninen, E.; Jungner, H. *Radiocarbon* **2001**, *43* (2A), 271–273.

(13) Lindroos, A.; Heienmeier, J.; Ringbom, A.; Brasken, M.; Sveinbojornstdottir, A. *Radiocarbon* **2007**, *49* (1), 47–67.

(14) Heinemeier, J; Jungner, H; Lindroos, A; Ringbom, A; von Konow, T; Rud, N *Nucl. Instrum. Methods Phys. Res., Sect. B* **1997**, *123*, 487–495.

(15) Pachiaudi, J. M.; Van Strydonk, M.; Dupas, M.; Dauchot-Dehon, M. *Radiocarbon* **1986**, *28* (2A), 691–697.

(16) Kosednar-Legenstein, B.; Dietzel, M.; Leis, A.; Stingl, K. *Appl. Geochem.* **2008**, *23*, 2425–2437.

(17) Van Strydonck, M.; Dupas, M.; Keppens, E. *Radiocarbon* **1989**, *31* (3), 610–618.

(18) Cazalla, O.; Rodriguez-Navarro, C.; Sebastian, E.; Cultrone, G. *J. Am. Ceram. Soc.* **2000**, *83* (5), 1070–1076.

(19) Bertolini, T.; Rubino, M.; Lubritto, C.; D'Onofrio, A.; Marzaioli, F.; Passariello, I.; Terrasi, F. *J. Mass Spectrom.* **2005**, *40* (8), 1104–1108.

(20) Zamba, I. C.; Stamatakis, M. G.; Cooper, F. A.; Themelis, P. G.; Zambas, C. G. *Mater. Charact.* **2007**, *58*, 1229–1239.

(21) Marzaioli, F.; Borriello, G.; Passariello, I.; Lubritto, C.; De Cesare, N.; D'Onofrio, A.; Terrasi, F. *Radiocarbon* **2008**, *50* (1), 139–149.

(22) McCrea, J. M. *J. Chem. Phys.* **1950**, *18*, 849–857.

(23) Rozanski, K.; Stichler, W.; Gonfiantini, R.; Scott, E. M.; Beukens, R. P.; Kromer, B.; van der Plicht, J. *Radiocarbon* **1992**, *34* (3), 506–519.

(24) McKinney, C. R.; McCrea, J. M.; Epstein, S.; Allen, H. A.; Urey, H. C. *Rev. Sci. Instrum.* **1950**, *21* (8), 724–730.

(25) Terrasi, F.; De Cesare, N.; D'Onofrio, A.; Lubritto, C.; Marzaioli, F.; Passariello, I.; Rogalla, D.; Sabbarese, C.; Borriello, G.; Casa, G.; Palmieri, A. *Nucl. Instrum. Methods Phys. Res., Sect. B* **2008**, *266*, 2221–2224.

(26) Stuiver, M.; Polach, H. A. *Radiocarbon* **1977**, *19* (3), 355–363.

(27) Stuiver, M., Reimer, P. J., Reimer, R. *CALIB Radiocarbon Calibration*, version 6.0; 2010, http://www.calib.org.

(28) Reimer, P. J., Reimer R. *CALIBomb Radiocarbon Calibration*, html program; 2010, http://www.calib.org

(29) Jenkyns, H. C.; Gale, A. S.; Corfield, R. M. *Geol. Mag.* **1994**, *131*, 1–34.

(30) Wissler, L.; Funk, H.; Weissert, H. *Palaeogeogr., Palaeoclimatol., Palaeoecol.* **2003**, *200*, 187–205.

(31) Zheng, L.; Xuehua, C.; Mingshu, T. *Cem. Concr. Res.* **1992**, *22* (1), 1–5.

(32) Paama, L.; Pitkanen, I.; Ronkkomaki, H.; Peramaki, P. *Thermochim. Acta* **1998**, *320* (1−2), 127–133.

(33) Elert, K.; Rodriguez-Navarro, C.; Pardo, E. S.; Hansen, E.; Cazalla, O. *Stud. Conserv.* **2002**, *47* (1), 62–75.

(34) McNaught, A. D. Wilkinson, A. In *Compendium of Chemical Terminology*, 2nd ed.; Blackwell Science: Oxford, U.K., 1997.

(35) Moropoulou, A.; Bakolas, A.; Aggelakopoulou, E. *Cem. Concr. Res.* **2001**, *31*, 633–639.